Near-Field Scanner for the Detection of Passive Intermodulation Sources in Base Station Antennas

Sami Hienonen, Viatcheslav Golikov, Pertti Vainikainen, *Member, IEEE*, and Antti V. Räisänen, *Fellow, IEEE*

***Abstract*—Passive intermodulation (PIM) distortion is a challenging problem in the design and manufacturing of base station antennas. Small nonlinearities, typically in junctions, may cause a distortion signal that interferes with the receiver even with a level of −155 dBc in a GSM900 system. The PIM level specification of an outdoor base station antenna is difficult to achieve and the sources of PIM generation are laborious to track down. In this paper, a near-field measurement method is presented to localize and investigate passive intermodulation sources in antennas and open transmission lines. The principle of the PIM near-field measurement is otherwise the same as in a common reactive near-field measurement, but instead of measuring the signal at the input frequency, the signal amplitude and phase at the PIM frequency of interest are acquired. The constructed measurement system is capable of measuring PIM signal levels down to −110 dBm with 2 × 43 dBm transmit power in the GSM900 frequency band. As demonstration measurements, PIM sources in a two-element base station antenna and in a microstrip line are localized.**

***Index Terms*—Base station antenna, near-field measurement, passive intermodulation, sensitivity.**

I. Introduction

PASSIVE intermodulation (PIM) is a phenomenon that can degrade the performance of a multichannel wireless communication system where the difference in the transmit and receive power is high. This degradation is due to nonlinear passive devices that generate interference signals at harmonic and intermodulation frequencies whenever two or more transmitting signals are present. Although passive devices such as cables, connectors, and antennas are usually considered as linear devices, they turn out to be slightly nonlinear when they are subject to high enough signal power. The origin of the distortion is typically either a nonideal contact in a junction or a nonlinear material in the RF path [1]–[3]. If the metal contact interfaces are oxidized, contaminated, rough, or they are loosely connected, the probability of getting excessive passive intermodulation distortion is considerably increased. There are many possible physical mechanisms that can cause the metal contact nonlinearity. These include the microdischarge through the microscopic voids in the metal structure, the tunnel, and the Schottky effect in the thin insulating film between the metals, and the electric breakdown through the dirt on the interfaces [4]–[6]. Ferromagnetic materials are known to produce PIM distortion levels on the order of magnitude greater than metal contacts [3]. Even stronger nonlinearity is found in ferrites, whose physical behavior is well known [7].

Passive intermodulation distortion has been found to cause problems in naval, spaceborne, and land communication systems [8]. Nowadays, as the mobile communication systems have become widespread, the passive intermodulation phenomenon has to be considered also in the base station antenna path components. Especially problematic is the GSM system, since the base stations use multiple simultaneous narrow-band carriers and their third-order intermodulation products fall to the receiving band. In a recent study, several commercial antennas were found to have a wide spread in their PIM characteristics [9]. Therefore, special attention must be paid to the design and fabrication of the GSM base station antennas. Although the PIM signal level of an antenna can be measured with dedicated analyzers, they do not give the information where the PIM distortion is generated. One can try to recognize the likely distortion sources, but verifying these assumptions is often very time consuming. Thus, an instrument that could localize a PIM source would be a valuable tool for an antenna designer both during the development as well as during the production phase of an antenna. Earlier, PIM sources have been detected in reflector antennas with microwave holographic imaging, in cables with a cable radar, as well as in base station towers and PIM chambers by illuminating the structures with high Tx power [10]–[13]. However, according to the knowledge of the authors, no method exists to localize PIM sources in a base station antenna.

In this paper, a near-field measurement method to localize PIM sources in open devices and structures such as microstrip lines and antennas is presented. The method is based on the idea that at the PIM frequency the reactive near field will have a discontinuity in the vicinity of the distortion source. It should be noted that there might be a field discontinuity also at the signal frequency, but this alone does not indicate that it is a source of PIM generation. In fact, typically these discontinuities in an antenna are easily identified visually. The actual problem is to examine which of them are causing the PIM distortion. Due to the measurement principle, PIM sources in closed components like cables and cavity filters cannot be located with this method. Antenna mounting structures could be measured, but the equipment described in this paper can be used only in a laboratory environment.

In the PIM scanner, two high-power Tx signals are fed to the antenna under test (AUT) which is scanned with either an electric- or a magnetic-field probe. The low PIM signal level (down to −117 dBm) sets stringent requirements for the probe and the

Manuscript received May 7, 2003; revised March 4, 2004. This work was supported in part by the Nokia Foundation, the Jenny and Antti Wihuri Foundation, the Emil Aaltonen Foundation, and the Academy of Finland and Tekes through their Center of Excellence Program.

The authors are with the Smart and Novel Radios Research Unit (SMARAD), Radio Laboratory, Helsinki University of Technology, FIN-02015 HUT, Finland (e-mail: Sami.Hienonen@hut.fi).

Digital Object Identifier 10.1109/TEMC.2004.837958

receiver residual intermodulation level. Earlier, this measurement method has been demonstrated for the GSM900 frequency band in [14] and the equipment sensitivity has been improved down to -110 dBm with Tx signals of 2×43 dBm [15]. In the current version of the hardware also the phase information of the PIM near-field component is measured, which allows the determination of the direction of the PIM source in a transmission line.

II. Passive Intermodulation Near-Field Scanner

A. Principle of the Measurement

The principle of the PIM near-field measurement is the same as in a common near-field measurement [16], [17]. The probe is moved very near to the DUT, typically at a distance smaller than one tenth of a wavelength. However, instead of measuring the signal at the input frequency, the signal at the PIM frequency of interest is measured. If the scanning area contains a PIM source, this is seen as a discontinuity in the measured data. Besides the near-field amplitude, the PIM near-field scanner is capable of measuring the PIM signal phase as well. Including the phase measurement has two advantages. Firstly, the noise floor is lowered by using coherent summing and secondly, the gradient of the phase points toward the direction of the PIM source in a transmission line. The latter characteristic extends the usability of the scanner, since the PIM source does not have to be included in the scanning area. It is sufficient to scan the both sides of the PIM source in order to localize it.

As in all PIM measurement equipment, the main problem of the measurement is the low PIM signal level compared to the Tx signals. In our case, the Tx signal levels at the AUT connector are 43 dBm, whereas the PIM signal sensitivity should be as low as -115 dBm. Especially, there are no published results what is the PIM behavior of near-field probes within high-field strengths. Therefore, various near-field sensors have been tested and extensive sensitivity measurements have been carried out in order to evaluate the equipment.

Typically, the PIM performance of a base station antenna is characterized in the reflection mode, where the reverse travelling PIM signal level is monitored. In order to get comparable results with this measurement, the measured near-field PIM data has to be normalized, see Fig. 1. The normalization also helps to distinguish a PIM source when the field distribution is not uniform as for example in a resonator. In the first measurement, the coupling between the AUT and the probe is determined; a known calibration signal $P_{\mathrm{cal,AUT}}$ at the PIM frequency is fed to the AUT and the field component is picked up by the probe, $P_{\mathrm{cal}}(x, y)$. In the second measurement, two high-power signals are fed to the AUT and the field strength at the PIM frequency is recorded, $P_{\mathrm{IM3}}(x, y)$. The normalized PIM near-field power is defined as

$$P_{\mathrm{IM3,AUT}}(x, y) = P_{\mathrm{IM3}}(x, y) - P_{\mathrm{cal}}(x, y) + P_{\mathrm{cal,AUT}}. \quad (1)$$

When the PIM source is located outside the scanning area, $P_{\mathrm{IM3,AUT}}(x, y)$ is constant and comparable with the reverse PIM level of the AUT. If the gain of the receiver G_{rec} is known,

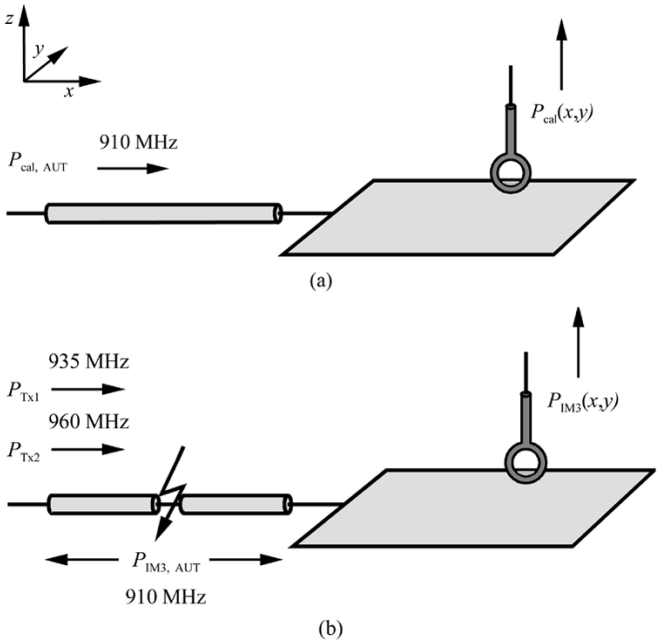

Fig. 1. Normalization of the PIM near-field measurement. (a) Small signal at 910 MHz is used as a calibration signal, $P_{\mathrm{cal,AUT}}$. (b) Two high-power Tx signals are fed to the AUT in the PIM signal measurement, P_{Tx1} and P_{Tx2}. A PIM source is located in the cable.

the coupling between the AUT and the probe can be calculated from the calibration signal measurement

$$C_{\mathrm{probe}}(x, y) = G_{\mathrm{rec}} - P_{\mathrm{cal}}(x, y) + P_{\mathrm{cal,AUT}}. \quad (2)$$

B. Description of the Equipment

The block diagram of the measurement equipment is shown in Fig. 2. The AUT, the receiver unit front end, and the linear guides are located inside a small shielded anechoic chamber. The receiver unit consists of a duplex filter, three Rx filters and three amplifiers. The Rx filters have at least 60 dB Tx signal attenuation each and two of them are placed outside the chamber so that possible Tx signal leakage from cables is filtered out. The PIM analyzer is used both as a high-power signal source and in monitoring the reverse PIM signal level. The PIM signal is picked up by the near-field probe, then filtered and amplified by the receiver unit. The duplex filter in the receiver is an essential component in terminating the Tx signals. Otherwise, there would be a standing wave in the probe cable, which would lead to unpredictable PIM distortion. Vector network analyzer (VNA) is used as the detector. By using coherent detection, the phase of the PIM signal can be measured and the sensitivity of the measurement is improved. The reference signal for the VNA is generated in the reference signal unit, which includes a mixer, amplifiers, filters and RF switches. A Tx signal sample is taken with a low-PIM 53-dB coupler. The reference signal unit is also used to inject the calibration signal $(P_{\mathrm{cal,AUT}})$ to the AUT. Both the stepping motors and the VNA are controlled by a computer. The PIM scanner operates in the GSM900 frequency band and its scanning range is 1.0×0.3 m^2.

The near-field probe has turned out to be the most critical part in the PIM near-field measurement. Although, the power level

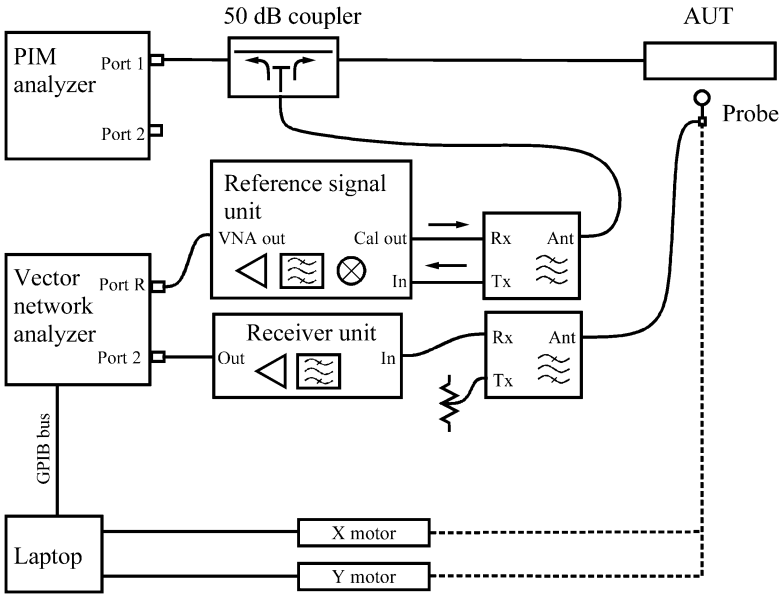

Fig. 2. Block diagram of the PIM near-field measurement equipment.

entering the probe is at most in the order of 23 dBm, the field strength is high enough to generate observable PIM distortion in the probe. Four different kinds of magnetic and three electric field probes have been constructed and tested during the development of the PIM scanner. The residual PIM level caused by the best probes was -115 dBm compared to the levels from -110 to -95 dBm of the other probes. As a result of the experiments, it can be summarized that the number of galvanic contacts must be minimized in the probes and special attention must be paid to the connection of the probe to the cable. Also, the properties of the outer surface of the probe seemed to affect the PIM level. Thus, the form of the probe should be smooth and and its surface should be flat and clean. The probe should have precise mechanical dimensions so that the contacts have a good fit and the soldering must be done properly. As usual, the probe and its contacts must be kept clean during and after the construction.

The best results have been achieved when the probes were realized with a flexible semirigid cable, e.g., Sucoform 141, which can be soldered to an N or 7/16 type connector (see Fig. 3). The magnetic field probe is made of a bent cable that forms a short-circuited loop and has a narrow gap in the outer conductor. This is a popular structure which has high E-field rejection. An extended inner conductor of the cable acts as the electric-field probe. The thick, rounded copper stub collects E-field power from wider range and lowers the E-field peak value at the probe, which improves the probe coupling and its PIM performance. However, semirigid cable like EZ 141 could have better performance as a magnetic field probe compared with the flexible semirigid. When a flexible semirigid cable is bent, micro-fractures can be formed in the wires of the outer conductor. This may increase the PIM level of the probe.

The reverse PIM signal level of the equipment with a low-PIM load as a termination was below -120 dBm with $P_{\mathrm{Tx}} = 2 \times 43$ dBm and $f_{\mathrm{IM3}} = 890$-915 MHz.

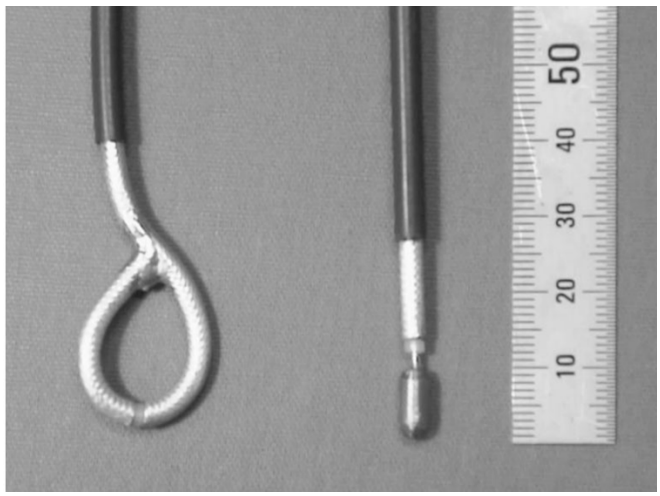

Fig. 3. Magnetic- and electric-field probes of the PIM scanner.

C. Sensitivity

Here, the sensitivity of the PIM scanner is defined to be the smallest detectable intermodulation signal power at the AUT, i.e., the smallest detectable $P_{\mathrm{IM3,AUT}}$. By definition, $P_{\mathrm{IM3,AUT}}$ depends on the coupling between the AUT and the probe so that it is a function of the probe location. An analysis and an evaluation of the various factors that limit the sensitivity of the PIM scanner have been described in [15]. It turned out that the sensitivity depends strongly on the 3-D location of the probe. There are three main causes for the sensitivity variation.

1) Thermal noise and low-level PIM limit the sensitivity in the locations of field minima.
2) Background PIM distortion generated in the surroundings of the AUT.
3) Self-generated PIM distortion of the probe near the metal edges of the AUT.

The measured noise density reduced to the input of the receiver is -172 ± 1 dBm/Hz.

Typical base station antennas behave as resonators, so that the electric and magnetic field strengths will have large variation over the antenna area. In the locations of field minima, either thermal noise or low-level PIM caused by the surroundings or by the probe may limit the sensitivity. The obvious way to circumvent this problem is to scan the AUT with both E- and H-field probes.

The background PIM distortion that is created in the surroundings of the AUT is caused by the chamber itself and the metal objects that belong to the scanner. Among others, these include the cabling, the linear guides and the receiver front end. Because the measurements have been carried out in a very small anechoic chamber ($2.5 \times 2.5 \times 2.5$ m^3), all the metal objects could not be covered with absorbers. The linear guides as well as the receiver front end had to be placed on the floor below the AUT, which points toward the ceiling. This restricts the usage of the scanner in its current configuration to the antennas that radiate to the half space. Anyway, measurements with a low-PIM antenna were done to test the PIM characteristics of the chamber with the metal objects inside. The antenna was moved in the x-direction with both x- and y-polarizations and a reverse PIM measurement was done with $P_{\mathrm{Tx}} = 2 \times 43$ dBm, $f_{\mathrm{IM3}} = 890$-915MHz. The maximum PIM level at each position ranged from -120 to -117 dBm. Only at one position, where the antenna was right over the linear guides off the table, the maximum level was -115 dBm. Thus, it is possible that the surroundings of the AUT limit the sensitivity of the measurement but no major contribution is expected.

It turned out that PIM distortion will be created in the probe itself when the probe is near the metal edges of the AUT. Hereafter, this effect will be called the edge effect. One explanation could be that this distortion is caused by other field components than the field component that is measured. For example, when measuring E_z-field, the horizontal field components E_x and E_y could cause the raised PIM levels. Between different probes, there are clear variations in the PIM signal levels caused by the edge effect. Thus, one can minimize the edge effect by a proper design of the probe.

The sensitivity of the scanner has been evaluated with a stacked patch antenna as the AUT, which has the reverse PIM level lower than -118 dBm with $P_{\mathrm{Tx}} = 2 \times 43$ dBm and $f_{\mathrm{IM3}} = 890$–915 MHz. Sensitivity measurement results with the E- and H-field probes can be seen in Fig. 4. The PIM signal power at the AUT is calculated from (1). In both the E and H-field scans some background PIM distortion is seen outside the antenna area. In the E-field scan, the higher PIM level at positions $x = \pm 100$ mm could be caused by the edge effect because the E_z has minima at those positions. There are also raised PIM levels along the line $x = 0$ mm. Here, the E_z field has a deep minimum. Closer look at the antenna center reveals that P_{IM3} is constant whereas P_{cal} has a minimum in the range from $x = -10$ to $+10$ mm. This suggests that the PIM is generated in the probe by the horizontal field components. In the H-field data, the PIM level is at most -115 dBm in the antenna area. In addition to background PIM, also thermal noise limits here the sensitivity at the edges of the scanning area.

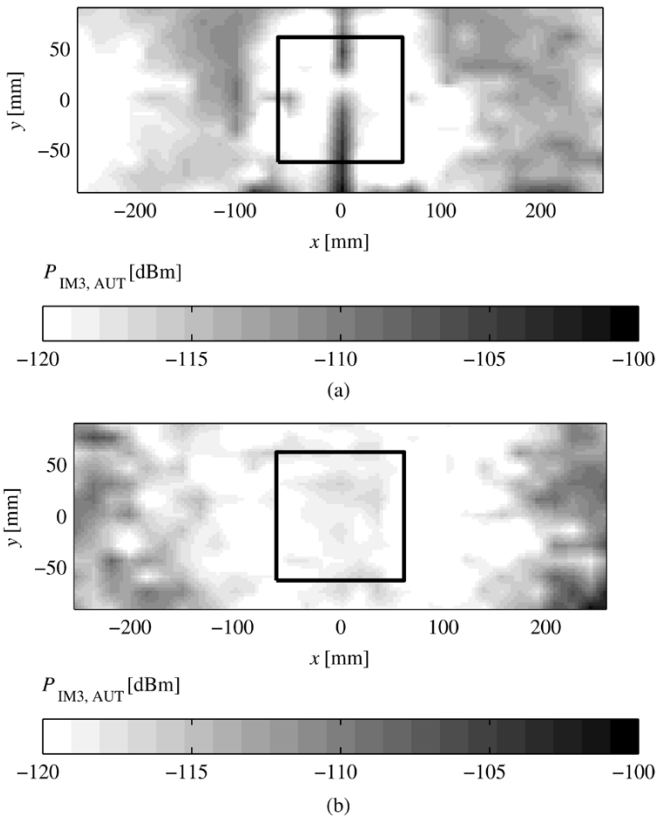

Fig. 4. PIM near-field scans of the reference antenna. The data is shown as normalized PIM level, $P_{\mathrm{IM3,AUT}}$, calculated from (1). Patch outline is drawn with a black line. Reverse PIM < -118 dBm, $P_{\mathrm{Tx}} = 2 \times 43$ dBm, $f_{\mathrm{IM3}} = 890$-915 MHz. Probe height from the antenna was 10 mm. (a) E_z-field scan. (b) H_y-field scan.

The normalized PIM level is mainly below -115 dBm in the reference antenna scans. Therefore, the scanner is capable of measuring PIM levels from -110 to -115 dBm, when the Tx signal power is 2×43 dBm. However, it must be kept in mind that the PIM level of the probe usually raises near the metal edges of the AUT and at the field minima. Therefore, comparison with the E- and H-field data can be helpful in interpreting the measurement results.

III. Measurements

All the measurements were carried out by using a Tx power of 2×43 dBm and frequencies of $f_1 = 935$ MHz and $f_2 = 960$ MHz. The third-order PIM signal at the frequency of $f_{\mathrm{IM3}} = 910$ MHz was recorded.

A. Two-Element Dipole Array

In order to test the performance of the PIM scanner, a commercial dual-polarized dipole antenna was measured. The antenna consists of four dipoles, so that two dipoles are connected parallel to each feed. Only the horizontal elements were excited in the measurements.

In the first setup the antenna was measured as it was. The reverse PIM of the antenna was -114 dBm, $P_{\mathrm{Tx}} = 2 \times 43$ dBm. The H_y-field scan shows that the normalized PIM level is relatively constant at about -110 dBm, Fig. 5. Only at the ends of the dipoles the PIM level is increased about 5 dB,

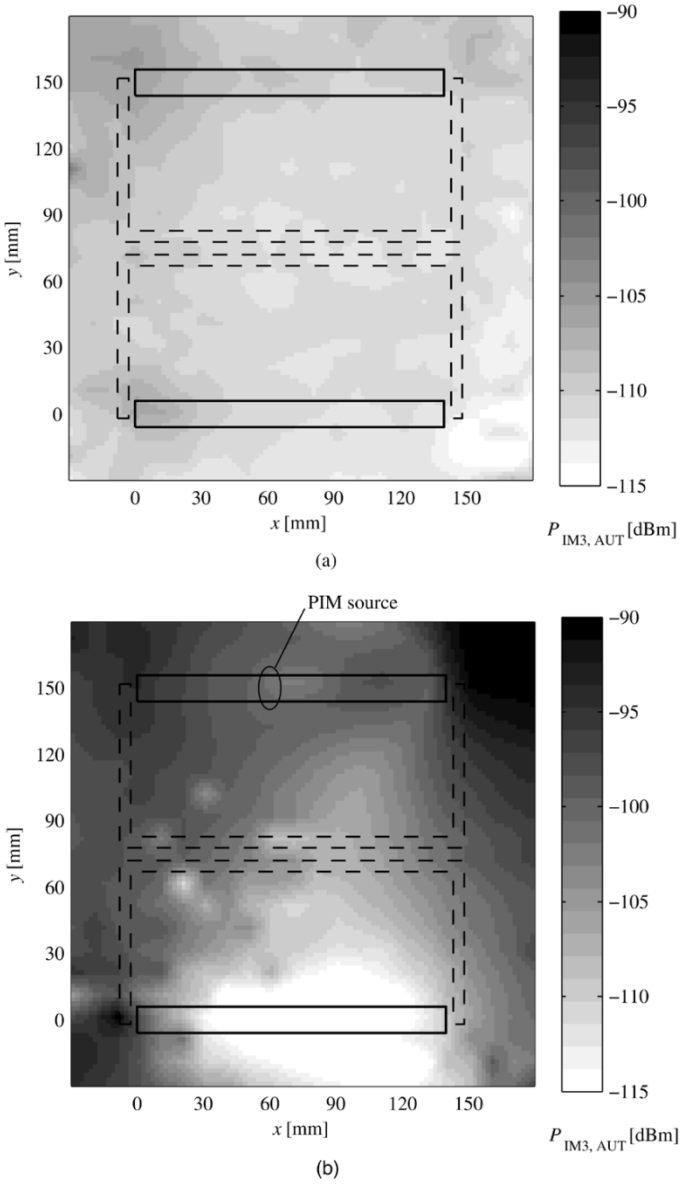

Fig. 5. H_y-field scan of the dipole antenna, $P_{\mathrm{IM3,AUT}}$. Outline of the dipoles is drawn with a black line. Probe height from the dipoles was 15 mm. (a) Unmodified antenna. Reverse PIM is -114 dBm. (b) Badly soldered feed in the upper dipole ($x = 60$ mm, $y = 150$ mm). Reverse PIM is -108 dBm.

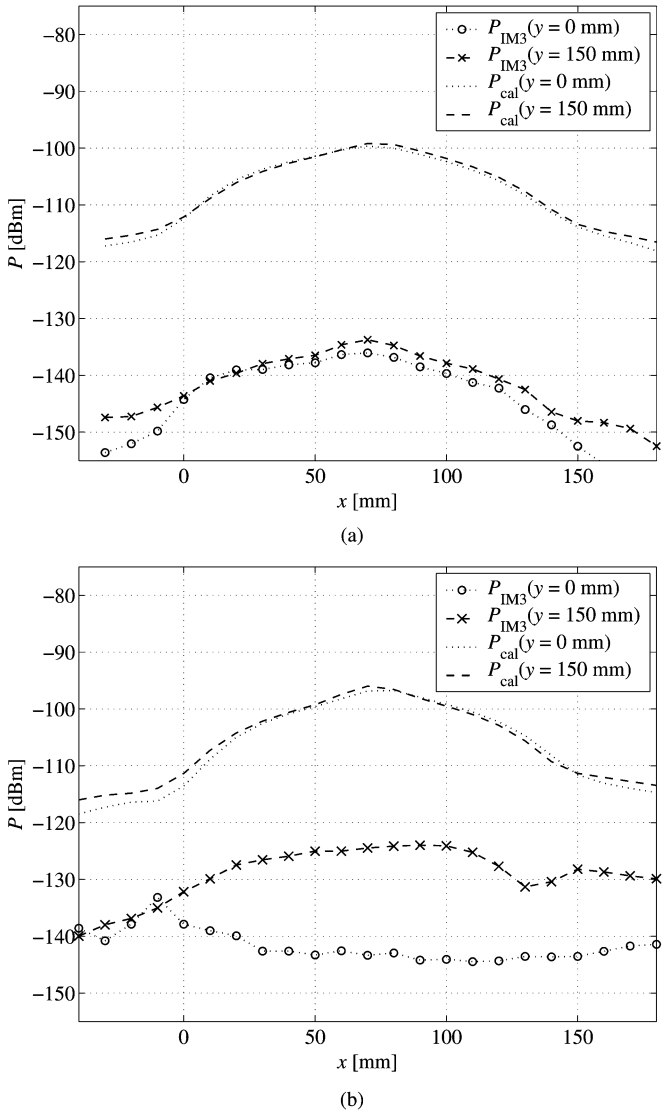

Fig. 6. H_y-field scan of the dipole antenna. P_{IM3} and P_{cal} entering the probe. (a) No PIM source. (b) PIM source at the upper dipole feed ($x = 60$ mm, $y = 150$ mm).

which implies the edge effect. The 4 dB difference between the reverse and the near-field PIM level could be explained by the unequal reverse and forward PIM. This difference cannot be explained by the self-generated PIM of the scanner since the ratio between P_{IM3} and P_{cal} is near 1 dB/dB over the whole scanning area. Thus, there does not seem to be PIM sources within the scanning area and the dipole elements perform equally well. After the first measurement, the feed of the upper dipole element ($x = 60$ mm, $y = 150$ mm), was resoldered with a poor quality so that the reverse PIM was increased to -108 dBm. The resulted H_y-field scan is shown in Fig. 5(b). Now, there is a clear difference between the different dipole elements. The PIM levels are considerably higher in the faulty element. However, the precise position of the PIM source cannot be seen because of the high Q factor of the dipole. Additionally, the dipole elements are connected to each other with a simple T-junction so that the PIM distortion created in the upper element is entered also to the lower element to some degree. It should be noted that the faulty solder junction in the upper element is not seen either in the return loss of the antenna nor in the calibration signal measurement, Fig. 6. It can be seen that P_{cal} remains the same between the original and the damaged antenna in both dipoles, which cannot be said about P_{IM3}. This measurement was carried out also with the E-field probe that gave similar results.

B. PIM Source in a Microstrip Line

The usefulness of the phase measurement was demonstrated with two scans of a 30-cm-long microstrip line with a PIM source. In the first example, the strip was constructed of two tin-copper sheets joined together with nylon screws. A piece of braided copper was inserted between the strip surfaces. This poor contact area (8×15 mm^2) acted as a PIM source, which generated a reverse PIM level of -87 dBm, $P_{\mathrm{Tx}} = 2 \times 43$ dBm.

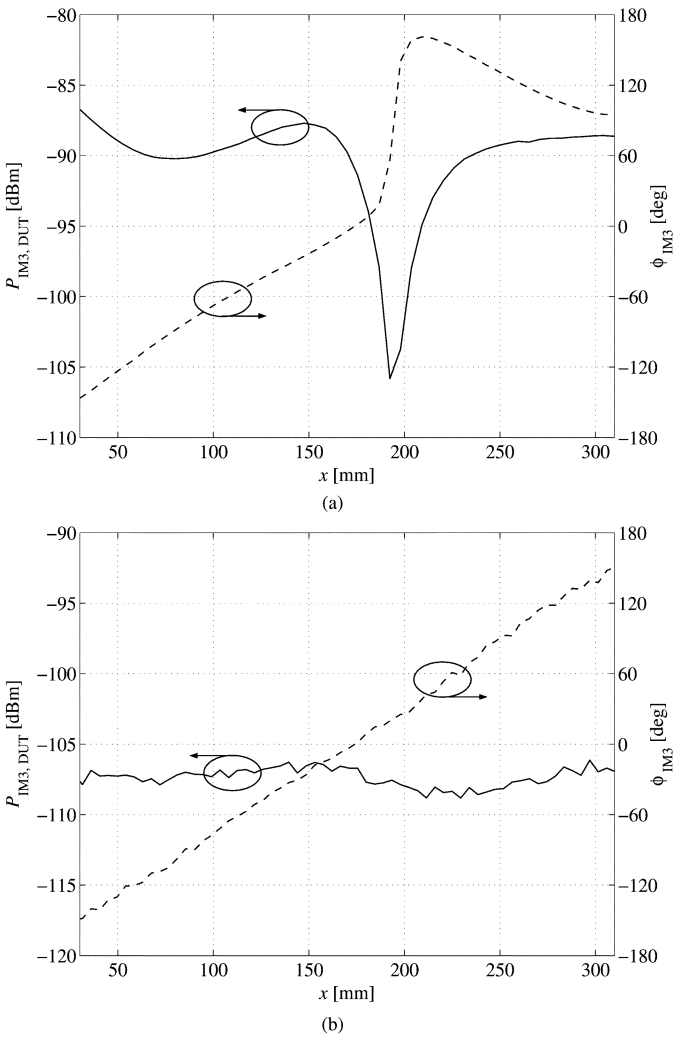

Fig. 7. PIM scans along the microstrip line. PIM phase, ϕ_{IM3}, and normalized PIM amplitude, $P_{\mathrm{IM3,DUT}}$. (a) PIM source at $x = 195$ mm, E-field scan. (b) PIM source is located outside the scanning range on the right-hand side of the plot, H-field scan.

In the second example, other connector of the microstrip acted as a PIM source with a reverse PIM level of -104 dBm.

The scan results are shown in Fig. 7. In the first scan, the PIM source at $x = 195$ mm is clearly seen in both amplitude and phase. The E_z-component has a minimum because the PIM source is in series with the strip so that the electric fields on the different sides of the PIM source are out-of-phase. This can be seen in the electric field phase that has approximately 150° jump in the vicinity of the source. Excluding the source area, the gradient of the phase points to the PIM source as was expected. The standing wave seen in the range of $x = 30$-180 mm of the $P_{\mathrm{IM3,DUT}}$ is caused by the 11 dB return loss of the PIM source. Thus, on the left side where the Tx signals come, the standing wave is present in the calibration measurement but not in the PIM measurement. In Fig. 7(b), the amplitude is essentially constant because the PIM source is not included within the scanning range. The PIM source resides on the right-hand side of the microstrip, which can be clearly seen from the phase. Although the exact position cannot be determined in this case, the knowledge of the direction of the PIM source is useful itself.

A fairly large PIM source in area has been used in the first experiment whereas also considerably smaller PIM sources occur in practise. Anyway, the size of the source is not crucial in the detection. Assuming that a small PIM source will not be seen in the amplitude data, the phase would anyway reveal its location. Also, the PIM phase helps to interpret measurement results in case of multiple PIM sources. The location of the PIM sources may be hidden in the resulting standing wave pattern with its minima and maxima in the amplitude. Thus, the actual PIM sources can be difficult to find from the amplitude data only.

IV. Conclusion

In this work, a passive intermodulation near-field scanner is described and its performance is evaluated. The scanner can detect PIM distortion levels in the AUT as low as -110 dBm with $P_{\mathrm{Tx}} = 2 \times 43$ dBm. However, near the metal edges of the AUT the PIM distortion created in the probe may deteriorate the scanner performance. The scanner has been used to localize PIM sources in a microstrip line and in a two-element dipole antenna. In the antenna, the exact position of the PIM source was not recovered but the faulty element was clearly identified. However, the PIM source localization in the microstrip line, which is a nonresonant structure, succeeded with an accuracy of less than one centimeter.

The implementation of the scanner is relatively straightforward to an existing PIM equipment. The construction of the probes is the most critical part in the PIM scanner development.

The PIM near-field scanner can be used to localize PIM sources in an open transmission line and to identify faulty elements in antenna arrays. Thus, it is believed that the scanner would be a useful tool in the process of the antenna design.

References

[1] F. Arazm and F. A. Benson, "Nonlinearities in metal contacts at microwave frequencies," *IEEE Trans. Electromagn. Compat.*, vol. 22, pp. 142–149, Aug. 1980.

[2] P. L. Lui and A. D. Rawlins, "Passive nonlinearities in antenna systems," in *Proc. IEE Colloquium Passive Intermodulation Products Antennas and Related Structures Tech. Dig.*, London, U.K., June 1989, pp. 6/1–6/7.

[3] J. S. Petit and A. D. Rawlins, "The impact of passive intermodulation on specifying and characterising components," in *Proc. 3rd ESA Electronic Components Conf.*, Noordwijk, The Netherlands, Apr. 1997, pp. 45–49.

[4] R. C. Chapman, J. V. Rootsey, and I. Polidi, "Hidden threat: Multicarrier passive component IM generation," in *Proc. AIAA/CASI 6th Communications Satellite Systems Conf.*, Montreal, QC, Canada, Apr. 1976, pp. 357–372.

[5] C. D. Bond, C. S. Guenzer, and C. A. Carosella, "Intermodulation generation by electron tunneling through aluminum-oxide films," *Proc. IEEE*, vol. 67, pp. 1643–1653, Dec. 1979.

[6] B. G. M. Helme, "Interference in telecomm systems, from passive intermodulation product generation: An overview," in *Proc. 22nd Antenna Measurement Techniques Association Annual Symp.*, Philadelphia, PA, Oct. 2000, pp. 143–149.

[7] Y.-S. Wu, W. H. Ku, and J. E. Erickson, "A study of nonlinearities and intermodulation characteristics of 3-port distributed circulators," *IEEE Trans. Microwave Theory Tech.*, vol. 24, pp. 69–77, Feb. 1976.

[8] P. L. Lui, "Passive intermodulation interference in communication systems," *Electron. Commun. Eng. J.*, vol. 2, pp. 109–118, June 1990.

[9] V. Golikov, S. Hienonen, and P. Vainikainen, "Passive intermodulation distortion measurements in mobile communication antennas," in *Proc. IEEE Vehicular Technology Conf.*, vol. 4, Atlantic, GA, Oct. 2001, pp. 2623–2625.

[10] P. L. Aspden, A. P. Anderson, and J. C. Bennett, "Microwave holographic imaging of intermodulation product sources applied to reflector antennas," in *Proc. 6th Int. Conf. Antennas Propagation*, Coventry, U.K., Apr. 1989, pp. 463–467.
[11] J. Siegenthaler and C. Stäger, "The measurement of microwave intermodulation effects on passive components and system parts," in *Microwaves Optoelectronics Conf.*, Wiesbaden, Germany, Mar. 1988.
[12] P. L. Lui and A. D. Rawlins, "The field measurement of passive intermodulation products," in *Proc. 5th Int. Conf. Mobile Radio Personal Communications*, Coventry, U.K., Dec. 1989, pp. 199–203.
[13] A. D. Rawlins, J. S. Petit, and S. D. Mitchell, "PIM characterization of the ESTEC compact test range," in *Proc. 28th European Microwave Conf.*, Amsterdam, The Netherlands, Oct. 1998, pp. 544–548.
[14] S. Hienonen, V. Golikov, V. S. Möttönen, P. Vainikainen, and A. V. Räisänen, "Near-field amplitude measurement of passive intermodulation in antennas," in *Proc. 31st European Microwave Conf.*, vol. 2, London, U.K., Sept. 2001, pp. 277–280.
[15] S. Hienonen, P. Vainikainen, and A. V. Räisänen, "Sensitivity measurements of a passive intermodulation near-field scanner," *IEEE Antennas Propagat. Mag.*, vol. 45, pp. 124–129, Aug. 2003.
[16] J. S. Dahele and A. L. Cullen, "Electric probe measurements on microstrip," *IEEE Trans. Microwave Theory Tech.*, vol. 28, pp. 752–755, July 1980.
[17] Y. Gao, A. Lauer, Q. Ren, and I. Wolff, "Calibration of electric coaxial near-field probes and applications," *IEEE Trans. Microwave Theory Tech.*, vol. 46, pp. 1694–1703, Nov. 1998.

Sami Hienonen was born in Helsinki, Finland, in 1970. He received the M.Sc. degree in technology and the Licentiate of Science in Technology degree from Helsinki University of Technology (HUT), Finland, in 1997 and 2000, respectively, and is currently working toward the Ph.D. degree in radio engineering.

Since 1997, he has been with the Radio Laboratory of HUT. His research interests include the design and measurement of microwave antennas and nonlinear effects in passive devices.

Viatcheslav Golikov was born in Tomsk, Russia, in 1978. He received the M.Sc. degree from Tomsk State University of Control Systems and Radioelectronics, Russia, in 1999, and the Licentiate of Science in Technology degree from Helsinki University of Technology (HUT), Finland, in 2003, where he is currently working toward the Ph.D. degree.

Since 1999, he has been a Researcher with the Radio Laboratory, Helsinki University of Technology, where, until 2003, he was a researcher. His main research interests are antennas, nonlinear effects in passive devices and their analysis.

Pertti Vainikainen (M'91) was born in Helsinki, Finland, in 1957. He received the M.Sc. degree in Technology, Licentiate of Science in Technology degree, and Doctor of Science in Technology degree from Helsinki University of Technology (HUT), Finland, in 1982, 1989, and 1991, respectively.

From 1992 to 1993, he was an Acting Professor, in 1993 he became an Associate Professor, and since 1998, he has been a Professor of Radio Engineering, Radio Laboratory of HUT. From 1993 to 1997, he was the director of the Institute of Radio Communications (IRC) of HUT. In 2000, he was a Visiting Professor at Aalborg University, Denmark. He is the author or co-author of three books and over 170 refereed international journal or conference publications and the holder of six patents. His main fields of interest include antennas and propagation in radio communications and industrial measurement applications of radio waves.

Antti V. Räisänen (S'76–M'81–SM'85–F'94) received the Doctor of Science (Tech.) degree in electrical engineering from the Helsinki University of Technology (HUT), Finland, in 1981.

He has held visiting scientist positions at the Five College Radio Astronomy Observatory (FCRAO), the University of Massachusetts, Amherst MA, Chalmers University of Technology, Gothenburg, Sweden, in the Department of Physics, University of California, Berkeley, at the Jet Propulsion Laboratory and the California Institute of Technology, Pasadena CA, and at the Paris Observatory and University of Paris 6. Currently, he is a Chair Professor of Radio Engineering, HUT, and is supervising research in millimeter wave components, antennas, receivers, and microwave measurements at HUT Radio Laboratory, and leads the Smart and Novel Radios Research Unit (SMARAD). In 1997, he was elected the Vice-Rector of HUT for the period of 1997–2000. He serves also as the Chairman of the Board of Directors of MilliLab (Millimeter Wave Laboratory of Finland—ESA External Laboratory). He has authored or co-authored more than 350 scientific or technical papers and six books, most recently *Radio Engineering for Wireless Communication and Sensor Applications* (Norwell, MA: Artech House, 2003).

Dr. Räisänen was the Chairman of the IEEE MTT/AP Chapter in Finland from 1987 to 1992. He was the Secretary General of the European Microwave Conference in 1982, served as the Conference Chair for the European Microwave Conference in 1992, and for the ESA Workshop on Millimeter Wave Technology and Applications in 1998. He was co-chair of the ESA Workshop on Millimeter Wave Technology and Applications in 2003. From 1995 to 1997, he served on the Research Council for Natural Sciences and Engineering, Academy of Finland. Currently, he serves as an Associate Editor of the IEEE TRANSACTIONS ON MICROWAVE THEORY AND TECHNIQUES.